Rainfall seasonality captured in micromammalian fauna in Late Quaternary contexts, South Africa

J. Francis Thackeray* & Jennifer M. Fitchett

Evolutionary Studies Institute, University of the Witwatersrand, Private Bag X3, WITS 2050, Johannesburg, South Africa

Received 11 April 2016. Accepted 14 July 2016

There exists ongoing debate regarding shifts in the latitudinal extent of the southern African winter-rainfall zone throughout the late Quaternary. Fossil proxies which can be related directly to rainfall seasonality have the potential to assist in quantifying these shifts. Relationships between mean monthly temperature and mean monthly rainfall in modern environments are quantified to generate a seasonality index associated with summer or winter rainfall. These seasonality indices can in turn be related to percentage occurrences reflecting relative abundances of rodent taxa represented in areas within southern Africa. Such data are used together to obtain an equation from which an index of seasonality in rainfall can be calculated, based on relative abundances of rodents in the modern landscape. The equation is applied to rodents represented in a Late Quaternary faunal sequence at Boomplaas Cave in the southeastern part of the Western Cape Province. Results confirm that this region experienced a predominantly winter-rainfall regime during the Last Glacial Maximum (LGM), though the amount of rain may have been relatively low for the coldest episodes *circa* 20 000 cal. yrs BP in the Boomplaas palaeo-environments.

Keywords: rainfall seasonality, Westerlies, microfauna, southern Africa, late Quaternary, Last Glacial Maximum.

INTRODUCTION

Situated at the intersection of the subtropical easterly and mid-latitude Westerly belts, southern African climate has a relatively unique boundary between clearly demarcated summer- and winter-rainfall zones (Chase & Meadows 2007; Chevalier & Chase 2015). The winter-rainfall zone, restricted at present to the southwestern Cape of South Africa, is controlled by the Westerlies, and notably the passage of frequent mid-latitude cyclones during winter months when the Inter-Tropical Convergence Zone shifts north (Barrable *et al.* 1998; Chevalier & Chase 2015). The summer-rainfall zone is influenced by a dominant high pressure cell throughout the winter months, and the intrusion of moist air from the Indian Ocean in summer (Carr *et al.* 2006; Mills *et al.* 2012). The resultant environment, and in particular the fauna, of the winter rainfall zone is thus markedly different from that of the interior, characterized by the rich fynbos centre of endemism (Mucina & Rutherford 2007). The most predominant synoptic scale changes that are likely to have occurred during the late Quaternary in South Africa are shifts in the position and strength of the Westerly belt, directly influencing the position of the winter-rainfall zone and associated flora, and indirectly influencing the degree of rainfall seasonality and rainfall patterns in the summer-rainfall zone (Chase & Meadows 2007; Norström *et al.* 2009; Stager *et al.* 2012).

The influence of the Westerlies in southern Africa during the late Quaternary has been of palaeoenvironmental interest for many decades, initiated by the work of Van Zinderen Bakker (1976) and Cockroft *et al.* (1987), who both argued for a considerable northward displacement of both the Westerly zone and of the influence of mid-latitude cyclones. More recent studies within the southern Cape of South Africa have led to some consensus that the strength of the Westerlies and the resultant winter-rainfall zone expanded in both northerly (Barrable *et al.* 1998; Chase & Meadows 2007; Stager *et al.* 2012) and easterly (Carr *et al.* 2006; Chase & Meadows 2007) directions, although the geographic limits of these shifts have yet to be quantified. This is due to difficulties in obtaining direct information pertaining to rainfall seasonality for a particular region from palaeoclimate proxies, which instead reflect broader fluctuations in total precipitation (Chase *et al.* 2015). Recent work presents quantified relative amounts of winter and summer rainfall for specific sites (Chase *et al.* 2015). Changes in the extent of the Westerly belt are not only of importance to the winter-rainfall zone, but also influence the frequency and intensity of mid-latitude cyclones in the interior regions of South Africa.

Existing attempts to reconstruct latitudinal shifts in the position of the Westerlies, and resultant changes in the region of influence of mid-latitude cyclones have predominantly relied on pollen assemblages (*cf.* Coetzee 1967; Norström *et al.* 2009) and climate modelling (Barrable *et al.* 1998; Mills *et al.* 2012). Pollen-based analyses rely on an assumption that the ratio of Poaceae to Asteraceae grains in a representative pollen count reflects the degree of seasonality of rainfall, with a greater Poaceae proportion

*Author for correspondence. E-mail: francis.thackeray@wits.ac.za

ZooBank: urn:lsid:zoobank.org:pub:55F96E3C-2346-4993-8E9D-E9E110326B0 (http://www.zoobank.org)
Permanently archived on the 11th of August 2016 at the University of the Witwatersrand, Johannesburg, South Africa.
The article is permanently archived at: http://hdl.handle.net/10539/20851

indicative of more pronounced summer-rainfall conditions (Coetzee 1967; Norström *et al.* 2009). Diatom and geochemical analyses have been used to explore changes in the amount of precipitation in the summer- (Stager *et al.* 2013) and winter-rainfall (Stager *et al.* 2012) zones, with implications for changes in rainfall seasonality discussed.

This paper proposes a method for identifying changes in rainfall seasonality during the Late Quaternary using fossil rodent abundances from late Quaternary sequences. A case study using fossil rodents from Boomplaas Cave, an archaeological site in the Western Cape of South Africa is used to assess the validity of the method. These results present the first rodent-based quantitative seasonality reconstruction for South Africa. A seasonality index is developed on the basis of the relationship between mean monthly temperature and mean monthly precipitation for South Africa, statistically segregating the contemporary winter rainfall areas which are characterized by an inverse relationship, and summer rainfall areas with positive relationships. These index values are then compared to the contemporary distribution of 12 rodent species common to the fossil record. This relationship, defined by a multiple regression model, is applied to fossil rodent distributions for a Late Quaternary sequence at Boomplaas cave in the southeastern region of the Western Cape published by Avery (1982), Deacon *et al.* (1984) and Thackeray (1987). From this, the rainfall seasonality at Boomplaas throughout the late Quaternary is quantified and temporal trends and cycles investigated.

METHODS

To determine the seasonal gradients across South Africa, a seasonality index was developed on the basis of the relationship between mean monthly temperature and mean monthly rainfall for a set of point locations across South Africa. Records of mean monthly temperature (MMT) and rainfall (MMR) records were obtained from the South African Weather Bureau for periods spanning 48–100 years, for 24 meteorological stations distributed across South Africa (Fig. 1), facilitating the exploration of rainfall to temperature ratios along north–south transects spanning the winter- to summer-rainfall zones. We quantify the seasonal relationship between MMR and MMT by the *m*-coefficient derived from the standard least squares linear regression equation $y = mx + c$, where y refers to the square-root transformed mean monthly rainfall values and x refers to the square-root transformed mean monthly temperature values.

The contemporary spatial distribution of 12 rodent species that are common to the Boomplaas fossil record and the contemporary microfauna of South Africa is determined using the De Graaff (1981) distribution maps, with relative percentage distributions determined for 31 grids at 2° latitude and longitude divisions locations across South Africa, all of which include meteorological stations from which temperature and rainfall measurements can be derived. These relative percentage distributions of each rodent species are then related statistically to the seasonality index score for each point location, defined by the position of the weather station. From this data, a multiple regression equation is developed of the form $m = b_0 + b_1x_1 + b_{2\times2}....b_nx_n$, where x_1, x_2....x_n reflect the relative abundance of each rodent taxon, expressed as percentage occurrences for each study area.

To quantify changes in late Quaternary moisture seasonality, the relative abundance of fossils from the same

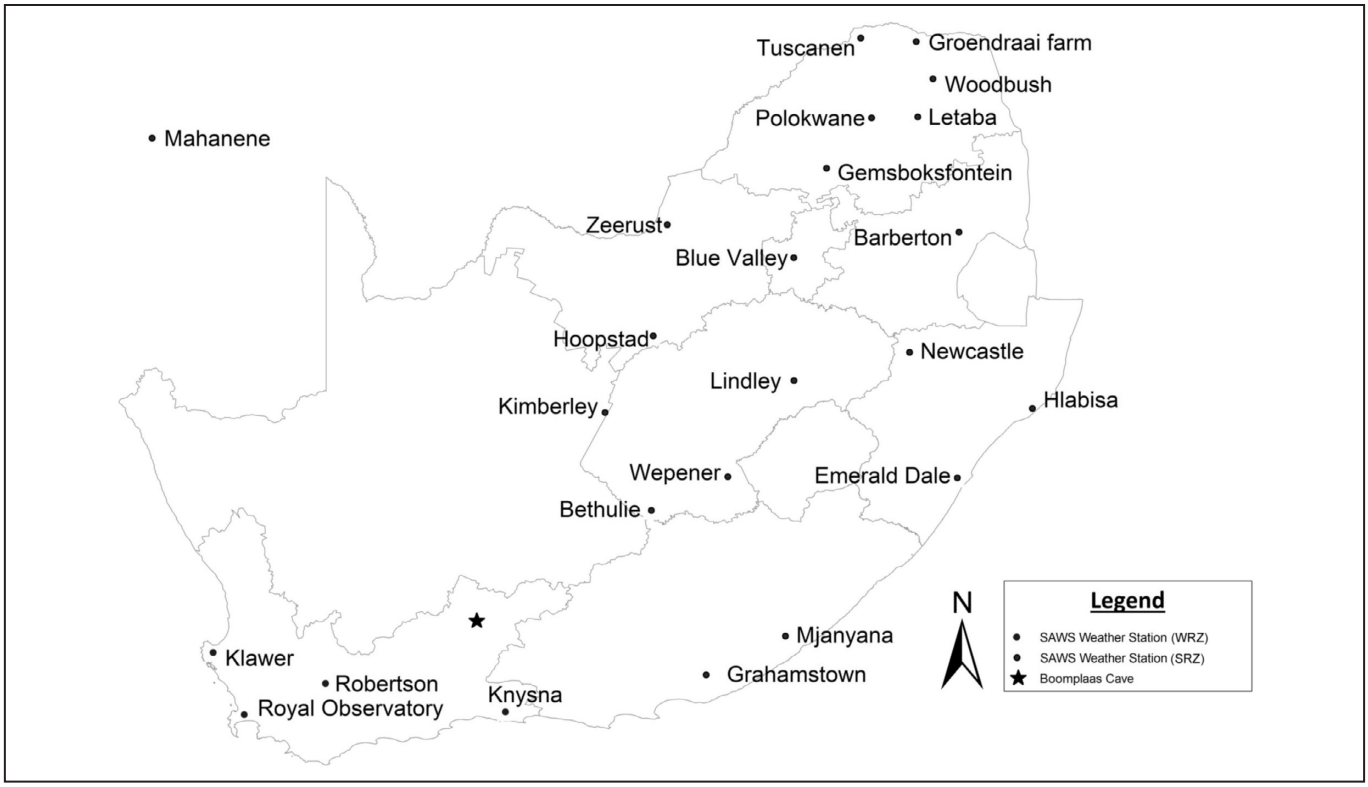

Figure 1. Map indicating the position of the South African Weather Service (SAWS) stations from which contemporary rainfall data were acquired. WRZ = winter rainfall zone; SRZ = summer rainfall zone.

group of 12 rodent fossils from the Boomplaas sequence is entered into the multiple regression model, providing a seasonality index output for each archaeological sample. A total of 12 samples have previously been dated on the basis of radiocarbon isotope analysis of charcoal, and are calibrated in this study using the ShCal13 calibration for the southern hemisphere. Dates for the remaining samples are interpolated using the BACON model, which employs millions of Markov Chain Monte Carlo simulations to provide estimates on the basis of depth, thickness and error margins (Blaauw & Christen 2011). These seasonality index scores calculated from the relative species distribution of rodent fossils from Boomplaas are plotted against age, using the C2 imaging software (Juggins 2007).

RESULTS

Positive values of the *m*-coefficient, or ratio, for MMT and MMR are associated with summer-rainfall regimes, whereas negative values are associated winter-rainfall regions such as Cape Town (Table 1). A value of 0 would indicate the hypothetical situation of equivalent year-round rainfall. The true 'year-round rainfall zone', encompassing much of the southern Cape of South Africa, has some seasonal variation in precipitation, with greater precipitation usually occurring in winter months than in summer. Selecting sites located in the winter rainfall zone (Cape Town), the classified year-round rainfall zone (Knysna), and two locations in the summer rainfall zone at progressively more northeasterly locations (Kimberly and Polokwane), the accuracy of this temperature: rainfall index in reflecting seasonality is confirmed (Fig. 2). The strongest negative *m*-value is obtained for Cape Town ($m = –0.93$), located close to the southernmost tip of Africa, in an undisputed winter-rainfall zone (Table 1, Fig. 2). The strongest positive score is calculated for Polokwane ($m = 1.79$), located in the northern interior of southern Africa (Fig. 2, Table 1). This particularly high *m*-score is driven in part by numerous summer months with zero rainfall; for regions in the northeastern interior, the greater moisture influx from the Indian Ocean moderates these scores somewhat. The variation in the strength and sign of the *m*-coefficient along a north–south gradient, and the dichotomy in sign between undisputed summer- and winter-rainfall zones of South Africa, confirms the application of this *m*-coefficient as a contemporary seasonality index.

It is then necessary to determine the spatial distribution of rodents, as these will be influenced, at least in part, by the temperature and precipitation patterns of a given location (Thackeray 1987; Root *et al.* 2003). The relative percentage distribution of the 12 rodents was determined from the De Graaff (1981) rodent distribution maps for southern Africa, for 2° latitude and longitude grids across South Africa and Namibia (Table 2). Examples of distribution maps for each of the rodents have been previously published (Thackeray 1987).

The contemporary spatial distribution of 12 species of rodents common to the Boomplaas sequence can be related to the *m*-coefficient using multiple regression analysis.

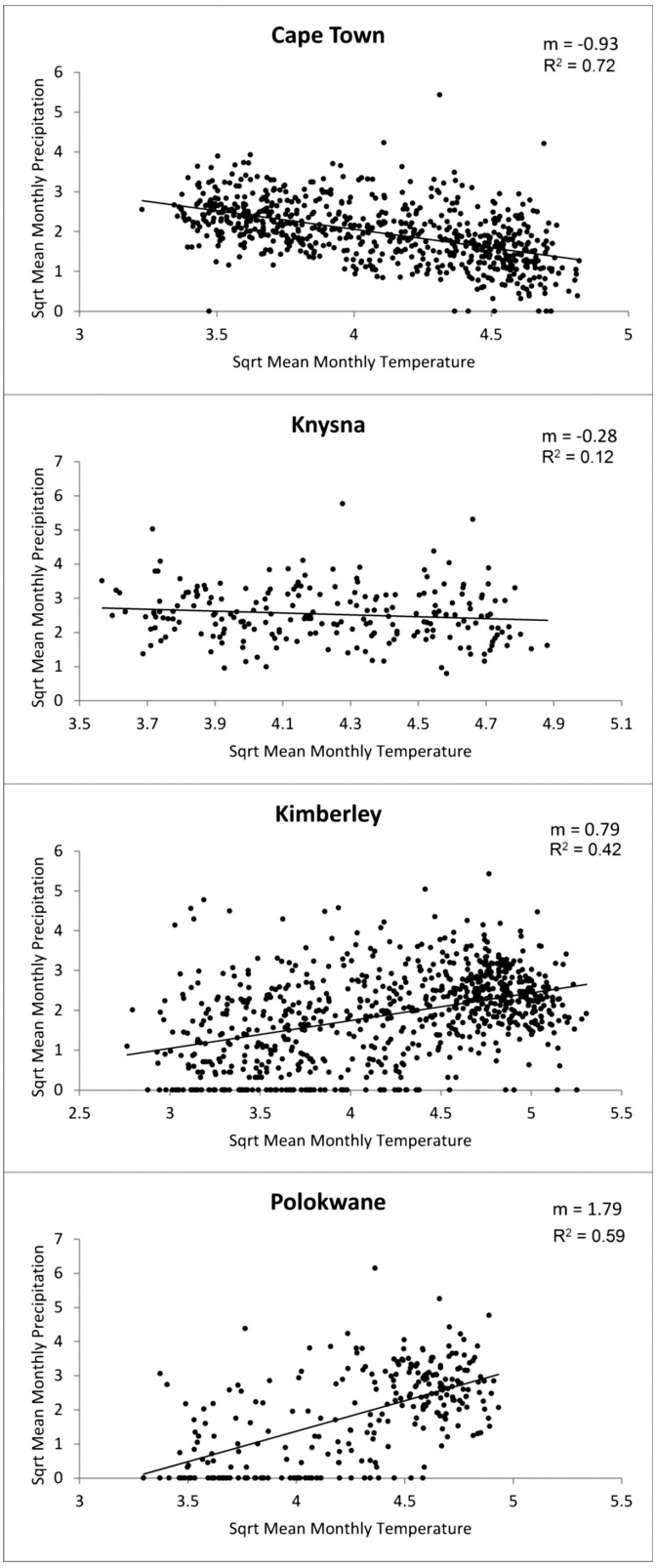

Figure 2. Relationships between square root transformed mean monthly rainfall (MMR) and mean monthly temperature (MMT) for four South Africa locations.

Input values for the calculation of this multiple regression model included the relative percentage distribution of each rodent type, and the rainfall:temperature ratio reflected by the regression term '*m*', for point locations designated at each of the 24 weather stations. The relationship between the *m*-coefficient and proxy measures of

Table 1. Seasonality index values for 20 stations in southern Africa (raw data from the South African Weather Services).

Weather station name and locality	Nearest town	Latitude (°S)	Longitude (°E)	Seasonality index value (*m*-coefficient)	Statistical strength (R^2)	Rainfall zone classification
Polokwane (South Africa)	Polokwane	23.9045	29.4689	1.79	0.59	Summer rainfall
Kimberley (South Africa)	Kimberley	28.7323	24.7623	0.79	0.42	Summer rainfall
Gemsboksfontein (South Africa)	Modimolle	28.4329	27.6740	0.706	0.96	Summer rainfall
Grahamstown (South Africa)	Grahamstown	33.3042	26.5328	0.513	0.82	Summer rainfall
Wepener (South Africa)	Wepener	29.7287	27.0381	0.456	0.96	Summer rainfall
Bethulie (South Africa)	Bethulie	30.4986	25.9746	0.455	0.95	Summer rainfall
Lindley (South Africa)	Bethlehem	27.8833	27.9167	0.380	0.98	Summer rainfall
Hoopstad (South Africa)	Bloemhof	27.8327	25.9083	0.270	0.88	Summer rainfall
Newcastle (South Africa)	Newcastle	27.7393	29.8762	0.260	0.98	Summer rainfall
Zeerust (South Africa)	Groot Marico	25.5370	26.0751	0.250	0.95	Summer rainfall
Emerald Dale (South Africa)	Port Shepstone	29.6833	29.4000	0.241	0.99	Summer rainfall
Barberton (South Africa)	Barberton	25.7884	31.0532	0.199	0.98	Summer rainfall
Mjanyana (South Africa)	Bisho	31.8378	28.1006	0.192	0.96	Summer rainfall
Letaba (South Africa)	Tzaneen	23.9000	30.0667	0.179	0.94	Summer rainfall
Groendraai Farm (South Africa)	Musina	24.1993	27.9848	0.167	0.89	Summer rainfall
Woodbush Forest (South Africa)	Louis Trichardt	23.7212	30.0572	0.167	0.95	Summer rainfall
Blue Valley (South Africa)	Johannesburg	25.9372	28.1152	0.157	0.78	Summer rainfall
Tuscanen (South Africa)	Mapungubwe	22.2075	29.2038	0.137	0.95	Summer rainfall
Hlabisa (South Africa)	Richards Bay	28.1452	31.8772	0.131	0.93	Summer rainfall
Mahanene (Namibia)	Ruacana	14.7830	17.4435	0.037	0.73	Summer rainfall
Klawer (South Africa)	Saldanha	31.7759	18.6250	–0.182	0.88	Winter rainfall
Knysna (South Africa)	Knysna	34.0366	23.0497	–0.28	0.12	Year round rainfall
Robertson (South Africa)	Robertson	33.8034	19.8854	–0.516	0.83	Winter rainfall
Royal Observatory (South Africa)	Cape Town	33.9258	18.4232	–0.93	0.72	Winter Rainfall

Table 2. Percentage distribution of the 12 rodent species for 31 locations across southern Africa interpolated from De Graaff's (1981) rodent distribution maps. *Aethomys namaquensis* **(ANAM),** *Cryptomys hottentotus* **(CHOT),** *Dendromus melanotis* **(DMEL),** *Mus minutoides* **(MMIN),** *Mystromys albicaudatus* **(MALB),** *Otomys irroratus* **(OIRR),** *Otomys laminatus* **(OLAM),** *Otomys saundersae* **(OSAU),** *Otomys unisulcatus* **(OUNI),** *Praomys natalensis* **(PNAT),** *Saccostomus campestris* **(SCAM) and** *Steatomys krebsi* **(SKRE).**

Latitude	Longitude	Province & country	CHOT	ANAM	MMIN	PNAT	MALB	DMEL	SKE	SCAM	OLAM	OSAU	OIRR	OUNI
18	14	Oshakati, Namibia	2.6	25.6	20.5	38.5	0.0	2.6	0.0	10.3	0.0	0.0	0.0	0.0
18	16	Oshana, Namibia	15.4	11.5	15.4	42.3	0.0	0.0	0.0	15.4	0.0	0.0	0.0	0.0
18	20	Runtu, Namibia	14.8	3.7	14.8	33.3	0.0	14.8	0.0	18.5	0.0	0.0	0.0	0.0
20	18	Otjozondjupa, Namibia	8.7	39.1	4.3	30.4	0.0	0.0	0.0	17.4	0.0	0.0	0.0	0.0
22	16	Erongo, Namibia	8.0	52.0	12.0	12.0	0.0	0.0	0.0	16.0	0.0	0.0	0.0	0.0
22	18	Windhoek, Namibia	10.3	34.5	0.0	24.1	0.0	0.0	0.0	31.0	0.0	0.0	0.0	0.0
22	20	Omaheke, Namibia	15.0	20.0	20.0	25.0	0.0	0.0	0.0	20.0	0.0	0.0	0.0	0.0
22	28	Limpopo, South Africa	10.6	42.6	6.4	19.1	0.0	0.0	0.0	21.3	0.0	0.0	0.0	0.0
24	28	Limpopo, South Africa	21.9	17.8	16.4	21.9	0.0	1.4	0.0	19.2	0.0	0.0	1.4	0.0
24	30	Limpopo, South Africa	12.2	14.6	13.4	36.6	0.0	4.9	0.0	11.0	1.2	0.0	6.1	0.0
24	32	Limpopo, South Africa	27.7	15.4	4.6	38.5	0.0	0.0	0.0	13.8	0.0	0.0	0.0	0.0
26	20	Kgalagadi, Namibia	44.0	16.0	20.0	0.0	0.0	12.0	0.0	8.0	0.0	0.0	0.0	0.0
26	26	North West, South Africa	14.8	21.3	4.9	23.0	6.6	9.8	1.6	9.8	0.0	0.0	8.2	0.0
26	28	Gauteng, South Africa	18.0	16.4	10.7	20.5	12.3	4.9	3.3	6.6	0.0	0.0	7.4	0.0
26	30	Limpopo, South Africa	10.9	15.6	10.9	39.1	1.6	6.3	0.0	1.6	1.6	0.0	12.5	0.0
26	32	Mpumalanga, South Africa	11.5	12.8	14.1	38.5	1.3	2.6	0.0	14.1	1.3	0.0	3.8	0.0
28	24	Northern Cape, South Africa	20.8	33.3	0.0	8.3	4.2	0.0	0.0	20.8	0.0	0.0	12.5	0.0
28	26	Bloemfontein, South Africa	20.7	13.8	15.5	29.3	12.1	3.4	1.7	3.4	0.0	0.0	0.0	0.0
28	28	Bloemfontein, South Africa	6.5	11.3	11.3	40.3	19.4	1.6	0.0	0.0	0.0	1.6	8.1	0.0
28	30	KwaZulu-Natal, South Africa	3.0	21.2	7.6	37.9	6.1	3.0	0.0	4.5	0.0	0.0	16.7	0.0
28	32	KwaZulu-Natal, South Africa	9.9	14.1	8.5	35.2	2.8	5.6	0.0	14.1	4.2	0.0	5.6	0.0
30	26	Free State, South Africa	18.0	20.0	10.0	22.0	8.0	2.0	0.0	8.0	0.0	2.0	8.0	2.0
30	28	Free State, South Africa	1.9	25.0	7.7	19.2	9.6	7.7	0.0	0.0	0.0	0.0	28.8	0.0
30	30	KwaZulu-Natal, South Africa	17.7	3.2	12.9	24.2	8.1	8.1	0.0	0.0	4.8	0.0	21.0	0.0
32	18	KwaZulu-Natal, South Africa	11.1	13.9	13.9	0.0	5.6	11.1	1.1	0.0	0.0	8.3	11.1	13.9
32	20	Northern Cape, South Africa	20.7	10.3	10.3	0.0	0.0	3.4	3.4	0.0	0.0	6.9	6.9	37.9
32	28	Eastern Cape, South Africa	12.3	8.8	12.3	26.3	12.3	0.0	0.0	5.3	0.0	10.5	12.3	0.0
33.5	22	Western Cape, South Africa	18.0	13.1	8.2	0.0	4.9	9.8	3.3	1.6	1.6	4.9	14.8	19.7
33.5	24	Eastern Cape, South Africa	20.0	16.7	10.0	3.3	3.3	3.3	3.3	6.7	0.0	0.0	10.0	23.3
33.5	26	Eastern Cape, South Africa	4.5	4.5	9.1	18.2	0.0	0.0	0.0	0.0	0.0	0.0	18.2	45.5
34	24	Western Cape, South Africa	9.4	9.4	6.3	20.3	3.1	3.1	0.0	9.4	0.0	7.8	14.1	17.2

relative abundances of modern rodent taxa, obtained from multiple linear regression analysis is given by:

m = 0.468ANAM + 0.474CHOT + 0.470DMEL + 0.468MMIN + 0.484MALB + 0.490OIRR + 0.419OLAM + 0.464OSAU + 0.467OUNI + 0.478PNAT + 0.487SCAM + 0.465SKRE – 47.353 (r = 0.758)

where the proxies for relative abundances of rodent taxa are percentage occurrences of the following taxa: *Aethomys namaquensis* (ANAM), *Cryptomys hottentotus* (CHOT), *Dendromus melanotis* (DMEL), *Mus minutoides* (MMIN), *Mystromys albicaudatus* (MALB), *Otomys irroratus* (OIRR), *Otomys laminatus* (OLAM), *Otomys saundersae* (OSAU), *Otomys unisulcatus* (OUNI), *Praomys natalensis* (PNAT), *Saccostomus campestris* (SCAM) and *Steatomys krebsi* (SKRE).

For validation purposes, this equation has been tested against climate datasets for a further 20 years for four locations, with a correlation in output described by Pearson's correlation coefficient at r = 0.89 (P > 0.001).

To explore the fluctuations in late Quaternary rainfall seasonality, this equation can be applied to the relative percentage distributions of fossil rodent assemblages throughout a quantified period of time. The fossil rodent assemblages from Boomplaas Cave (Avery 1982; Deacon *et al.* 1984; Thackeray 1987) were selected due to the high quality of preservation, and the position of the cave at the southwestern-most border of the summer rainfall zone. The proportional distribution of the rodent species was determined from 38 archaeological samples from the Boomplaas excavation, as detailed by Thackeray (1987). Radiocarbon dates were available for 12 samples, as outlined in Table 3. Dates were calibrated using ShCal13, and for the remaining samples, age–depth interpolations were made using the BACON model (Fig. 3). The sequence is confirmed to span the late Quaternary from ~80 000 cal. yrs BP to present, with high sample resolution spanning the LGM, terminal Pleistocene and Holocene (Fig. 3).

The multiple regression equation relating the contemporary rodent distribution to the contemporary rainfall seasonality is then applied to these microfaunal data. The m-coefficient for each sample, derived from the multiple regression equation, is plotted against age (Fig. 4), to deter-

Table 3. Radiocarbon dates for the samples used in the palaeoenvironmental reconstruction presented in this study. Conventional dates calibrated using ShCal13.

Sample number	Sample name	Top depth (m)	Bottom depth (m)	Laboratory code	Radiocarbon date (yr BP)	Uncertainty (yr)
50	DGLL1	0.28	0.42	UW-337	1 630	50
52	BLD2	0.82	0.83	UW-338	1 700	50
57	BLA	0.88	0.97	UW-306	6 400	75
59	BRL2	1.10	1.21	UW-410	9 100	135
63	BRL6	1.26	1.30	UW-411	10 425	125
65	CL1	1.30	1.40	Pta-1828	12 060	105
67	CL3	1.50	1.60	UW-301	14 200	240
68	GWA	1.60	1.67	Pta-3283	17 830	180
73	LPC2CB	2.03	2.23	UW-300	21 110	420
76	YOL	2.23	2.63	UW-304	32 400	700
80	OLP1	3.10	3.17	Pta-1811	37 390	1370
81	OLP2	3.18	3.30	UW-305	40 000	Radiocarbon limit

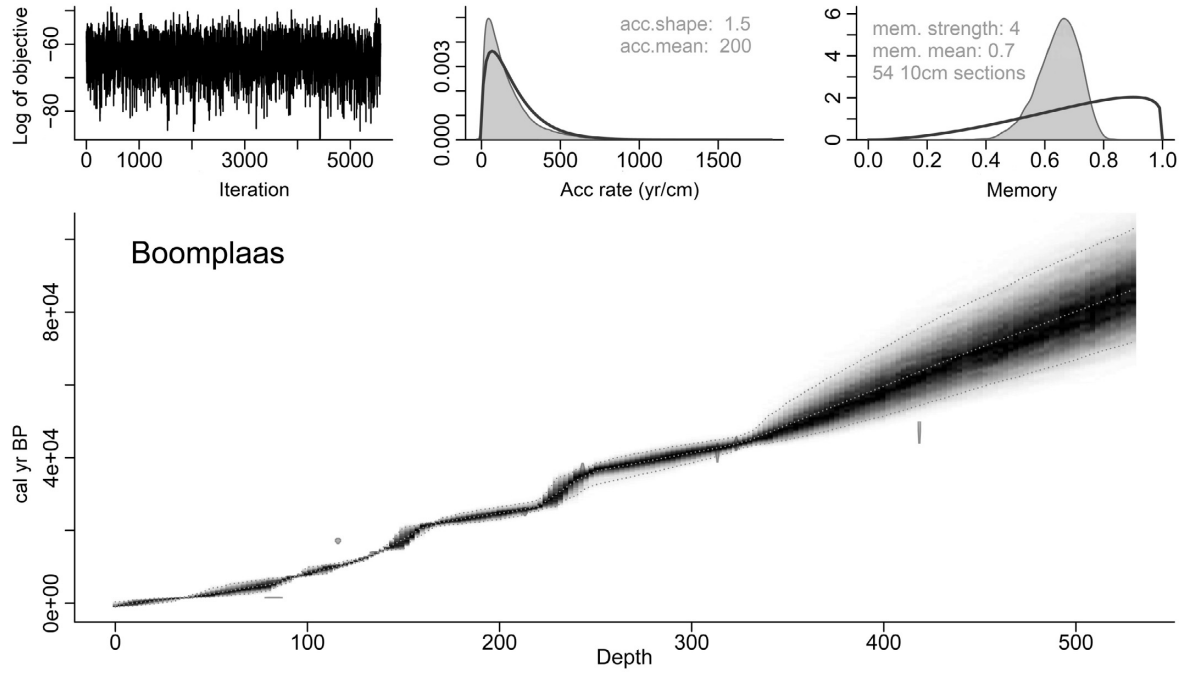

Figure 3. Age–depth output from the BACON model.

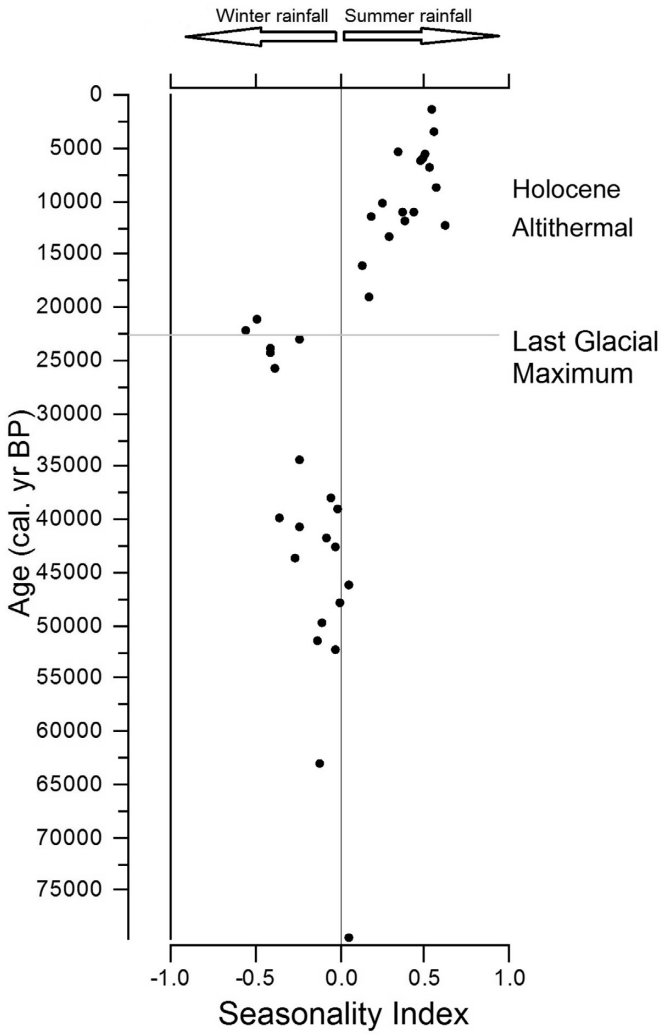

Figure 4. Temporal variability in rainfall seasonality calculated from the relative abundances of rodents at Boomplaas Cave, based multiple regression analysis of rodent data and *m*-coefficient based on modern climatic statistics.

mine fluctuations in rainfall seasonality at Boomplaas Cave throughout the late Quaternary. A notable shift from negative to positive *m*-coefficient scores is notable at ~19 200 cal. yrs BP; coinciding with the termination of the LGM. The strongest negative scores (m = –0.403 – m = –0.546) are calculated from ~23 940–21 270 cal. yrs BP (Fig. 4); coinciding with the coldest period of the LGM (Scott 1999). The *m*-coefficient scores increase throughout the terminal Pleistocene and early Holocene to a sustained peak (m = 0.542 – m = 0.573) from ~8840–7030 cal. yrs BP (Fig. 4), potentially indicating the Holocene Altithermal (Neumann *et al.* 2014). Following fluctuations in the mid- to late-Holocene, sustained strong positive scores mark the period 3360 cal. yrs BP to present (Fig. 4). It should also be noted that for much of the late Pleistocene period from ~80 000 cal. yrs BP – 39 050 cal. yrs BP, the seasonality index scores were very close to zero (Fig. 4), indicating that the site would have been characterized by year-round rainfall with no distinct seasonality.

DISCUSSION AND CONCLUSIONS

Following Van Zinderen Bakker (1974) and Tyson's (1986) models of southern African climatic change, periods of increased winter rainfall are associated with a northward displacement of the Westerlies. Microfauna results from Boomplaas indicate a striking difference in rainfall seasonality before and after the LGM. The strongest negative seasonality index values coincide with the LGM (Fig. 3), indicating that during this period, the climate at Boomplaas was characterized by winter-rainfall conditions when temperatures may have been at least 5°C lower than modern conditions. (Partridge 1999; Holmgren *et al.* 2003). This is supported by findings from glacial moraines in eastern Lesotho (Mills *et al.* 2012), and pollen and diatom results for Braamhoek Wetland in the Free State (Norström *et al.* 2009; 2014).

Seasonality index scores close to zero, indicating low seasonality of rainfall similar to that of the contemporary year-round rainfall zone are noted prior to the LGM, with stronger negative seasonality index scores from ~63 100–49 900 cal. yrs BP (Fig. 4). There is an abrupt shift to positive seasonality index scores at ~19 210 cal. yrs BP (Fig. 4), indicating a rapid shift from winter-rainfall to summer-rainfall conditions at Boomplaas. Summer-rainfall to year-round-rainfall conditions characterize the climate of the site today. The rainfall seasonality index correlates closely with inferred changes in temperature for Boomplaas (Thackeray 1987). The seasonality chronology presented here is notably also similar to climatic reconstructions for Seweweekspoort (Chase *et al.* 2013) and Cango Caves (Talma & Vogel 1992), both located in close proximity to Boomplaas. This association would suggest that changes in the seasonality index for the Pleistocene/Holocene transition may be attributable to displacements in the Westerlies (Chase *et al.* 2013; Chevalier & Chase 2015). However, low moisture index values for Boomplaas samples inferred from rodent fossils from units dated from ~23 940–21 270 cal. yrs BP, provide good evidence for relatively dry conditions in comparison with Holocene climates in the same region. If equator-ward displacement of the Westerlies brought more winter rainfall to the southern Cape during the LGM, it is probable that moisture availability for plant and animal growth may have been limited during this period (Mills *et al.* 2012).

Notably, Chase *et al.* (2013) highlight a pronounced dry period from 7–5 cal. yrs BP, which they associate with a southward retreat of the Westerlies. The seasonality index for Boomplaas indicates a period of strongest positive scores from ~8840–5720 cal. yrs BP (Fig. 4), which reflecting more pronounced summer-rainfall conditions, would similarly require a southward displacement of the Westerlies. This is followed by significantly reduced seasonality index values at Boomplaas, which are largely consistent with the reduced temperatures at Cango Cave (Talma & Vogel 1992; Stute & Talma 1998), as a reduction strong summer-rainfall seasonality would be associated with a northward return of the Westerlies, and an increased incidence of mid-latitude cyclones and associated cold front conditions. The seasonality chronology for Boomplaas is also largely consistent with climate reconstructions for what Chevalier & Chase (2015) define as the region influenced predominantly by shifts in the Westerlies. The timing of the shift in seasonality marking the termination of the LGM is consistent with that for the South Atlantic,

occurring earlier than for the regions dominated by the warmer Indian Ocean (Sonzogni *et al.* 1998).

Proxy-based climate reconstructions are inherently limited in their accuracy due to the complexity of environmental factors which control the proportional abundances of sub-groups of the proxy (Jackson 2012; Juggins 2013). It is therefore difficult to assign a trend specifically to a unique climate driver, rather than to the more complex interrelationship of climatic and non-climatic forces (Juggins 2013). It is for this reason that this study begins with modelling patterns in rainfall seasonality across South Africa from contemporary multi-decadal meteorological records. These records are then related to the contemporary spatial distribution of a group of rodents consistent with those in the fossil record. In so doing, a transfer function is developed, improving the accuracy from more qualitative interpretations from the fossil assemblages alone (Fritz *et al.* 1991; Stevenson & Pan 2004; Juggins 2013)

This study makes two significant contributions to improved understanding of late Quaternary variations in South African rainfall seasonality, and causal shifts in the Westerlies. At a broad scale, this study responds to the continued call for, and attempts in finding, proxies of palaeoclimatic rainfall seasonality in southern Africa (*cf.* Van Zinderen Bakker 1976; Barrable *et al.* 1998; Chase & Meadows 2007; Stager *et al.* 2012), by presenting the application of fossil microfauna. More specifically, through the application of this approach, this study confirms winter-rainfall conditions at Boomplaas during the LGM, associated with lowered mean annual precipitation, and a transition to summer-rainfall conditions at the termination of the LGM, which persist throughout the Holocene This contributes to improving the understanding of regional rainfall variability during the LGM and particularly under periods of shifts in the extent of the Westerlies. While it is a challenge to try to integrate data from micromammals (in this case rodents and insectivores) with climatic data, we believe that this approach provides a valuable contribution to the reconstruction of rainfall seasonality throughout the late Quaternary. Moreover, in this particular instance, the data reveal that winter rainfall during the time of the Last Glacial Maximum in the southern Cape coincided with limited precipitation, such that cold, dry conditions prevailed.

This work was supported by the National Research Foundation and the Andrew Mellon Foundation through grants awarded to J.F.T., and the DST/NRF Centre of Excellence for Palaeosciences through grants awarded to J.M.F.

REFERENCES

AVERY, D.M. 1982. Micromammals as palaeoenvironmental indicators and an interpretation of the late Quaternary in the southern cape province, South Africa. *Annals of the South African Museum* **8**, 183–374.

BARRABLE, A., MEADOWS, M.E. & HEWITSON, B.C. 1998. Environmental reconstruction and climate modelling of the Late Quaternary in the winter rainfall region of the Western Cape, South Africa. *South African Journal of Science* **98**, 611–616.

BLAAUW, M. & CHRISTEN, J.A. 2011. Flexible paleoclimate age–depth models using an autoregressive gamma process. *Bayesian Analysis* **6**(3), 457–474.

CARR, A.S., THOMAS, D.S.G., BATEMAN, M.D., MEADOWS, M.E. & CHASE, B. 2006. Late Quaternary palaeoenvironments of the winter-rainfall zone of southern Africa: Palynological and sedimentological evidence from the Agulhas Plain. *Palaeogeography, Palaeoecology, Palaeoclimatology* **239**, 147–165.

CHASE, B.M. & MEADOWS, M.E. 2007. Late Quaternary dynamics of southern Africa's winter rainfall zone. *Earth Science Reviews* **84**, 103–138.

CHASE, B.M., BOOM, A., CARR, A.S., MEADOWS, M.E. & REIMER, P.J. 2013. Holocene climate change in southernmost South Africa: rock hyrax middens record shifts in southern westerlies. *Quaternary Science Reviews* **82**, 199–205.

CHASE, B.M., LIM, S., CHEVALIER, M., BOOM, A., CARR, A.S., MEADOWS, M.E. & REIMER, P.J. 2015. Influence of tropical easterlies in southern Africa's winter rainfall zone during the Holocene. *Quaternary Science Reviews* **107**, 138–148.

CHEVALIER, M. & CHASE, B.M. 2015. Southeast African records reveal a coherent shift from high- to low-latitude forcing mechanisms along the east African margin across last glacial–interglacial transition. *Quaternary Science Reviews* **125**, 117–130.

COCKROFT, M.J., WILKINSON, M.J. & TYSON, P.D. 1987. The application of a present-day climatic mode to the Late Quaternary in southern Africa. *Climatic Change* **10**, 161–181.

COETZEE, J.A. 1967. Pollen analytical studies in East and southern Africa. *Palaeoecology of Africa* **3**, 1–146.

DEACON, H.J., DEACON, J., SCHOLTZ, A., THACKERAY, J.F., BRINK, J.S. & VOGEL, J.C. 1984. Correlation of palaeoenvironmental data from the late Pleistocene and Holocene deposits at Boomplaas cave, Southern Cape. **In**: J.C. Vogel (ed.), Late Cainozoic Palaeoclimates of the Southern Hemisphere, 339–352. Rotterdam, Balkema.

DE GRAAFF, G. 1981. *The Rodents of Southern Africa.* Durban, Butterworths.

FRITZ, S.C., JUGGINS, S., BATTARBEE, R.W. & ENGSTRUM, D.R. 1991. Reconstruction of past changes in salinity and climate using a diatom-based transfer function. *Nature* **352**, 706–708.

HOLMGREN, K., LEE-THORP, J.A., COOPER, G.R.J., LUNDBLAD, K., PARTRIDGE, T.C., SCOTT, L., SITHALDEEN, R., TALMA, A.S. & TYSON, P.D. 2003. Persistent millennial-scale climatic variability over the past 25 000 years in southern Africa. *Quaternary Science Reviews* **22**, 2311–2326.

JACKSON, S. 2012. Representation of flora and vegetation in Quaternary fossil assemblages: known and unknown knowns and unknowns. *Quaternary Science Reviews* **49**, 1–15.

JUGGINS, S. 2007. C2, Software for ecological and palaeoecological data analysis and visualisation, User guide Version 1.5. Retrieved on 11 July 2014 from www.staff.ncl.ac.uk/stephen.juggins/software/code/C2.pdf

JUGGINS, S. 2013. Quantitative reconstructions in palaeolimnology: new paradigm or sick science? *Quaternary Science Reviews* **64**, 20–32.

MILLS, S., GRAB, S., REA, B., CARR, S. & FARROW, A. 2012. Shifting westerlies and precipitation patterns during the Late Pleistocene in southern Africa determined using glacier reconstruction and mass balance modelling. *Quaternary Science Reviews* **55**, 145–159.

MUCINA, L. & RUTHERFORD, M.C. 2006. *The Vegetation of South Africa, Lesotho and Swaziland*. Cape Town, South African National Biodiversity Institute.

NEUMANN, F.H., BOTHA, G.A. & SCOTT, L. 2014. 18,000 years of grassland evolution in the summer rainfall region of South Africa: evidence from Mahwaqa Mountain, KwaZulu-Natal. *Vegetation History and Archaeobotany* **23**(6), 665–681.

NORSTRÖM, E., SCOTT, L., PARTRIDGE, T., RISBERG, J. & HOLMGREN, K. 2009. Reconstruction of environmental and climate changes at Braamhoek wetland, eastern escarpment South Africa, during the last 16 000 years with emphasis on the Pleistocene–Holocene transition. *Palaeogeography, Palaeoecology, Palaeoclimatology* **271**(3), 240–258.

NORSTRÖM, E., NEUMANN, F.H., SCOTT, L., SMITTENBERG, R.H., HOLMSTRAND, H., LUNDQVIST, S., SNOWBALL, I., SUNDQVIST, H.S., RISBERG, J. & BAMFORD, M. 2014. Late Quaternary vegetation dynamics and hydro-climate in the Drakensberg, South Africa. *Quaternary Science Reviews* **105**, 48–65.

PARTRIDGE, T.C., SCOTT, L. & HAMILTON, J.E. 1999. Synthetic reconstructions of southern African environments during the Last Glacial Maximum (21–18 kyr) and the Holocene altithermal (8–6 kyr). *Quaternary International* **57/58**, 207–214.

ROOT, T., PRICE, J., HALL, K., SCHNEIDER, S., ROSENZWEIG, C. & POUNDS, J. 2003. Fingerprints of global warming on wild animals and plants. *Nature* **421**, 57–60.

SCOTT, L. 1999. Vegetation history and climate in the Savanna biome South Africa since 190,000 ka: a comparison of pollen data from the Tswaing Crater (the Pretoria Saltpan) and Wonderkrater. *Quaternary International* **57/58**, 215–223.

SONZOGNI, C., BARD, E. & ROSTEK, F. 1998. Tropical sea-surface temperatures during the last glacial period: a view based on alkenones in Indian Ocean sediments. *Quaternary Science Reviews* **17**, 1185–1201.

STAGER, J.C., MAYEWSKI, P.A., WHITE, J., CHASE, B.M., NEUMANN, F.H., MEADOWS, M.E., KING, C.D. & DIXON, D.A. 2012. Precipitation variability in the winter rainfall zone of South Africa during the last 1400 yr linked to the austral westerlies. *Climate of the Past* **8**, 877–887.

STAGER, J.C., RYVES, D.B., KING, C., MADSON, J., HAZZARD, M., NEUMANN, F.H. & MAUD, R. 2013. Late Holocene precipitation variability in the summer rainfall region of South Africa. *Quaternary Science Reviews* **67**, 105–120.

STEVENSON, R.J. & PAN, Y. 2004. Assessing environmental conditions in rivers and streams with diatoms. **In**: E.F Stoermer & J.P. Smol (eds), *The Diatoms: Applications for the Environmental and Earth Science*, 11–40. Cambridge, Cambridge University Press.

STUTE, M. & TALMA, A.S. 1998. Glacial temperatures and moisture transport regimes reconstructed from noble gas and d18O, Stampriet aquifer, Namibia. **In**: *Isotope Techniques in the Study of Past and Current Environmental Changes in the Hydrosphere and the Atmosphere*, 307–328 IAEA Vienna Symposium 1997, Vienna.

TALMA, A.S. & VOGEL, J.C. 1992. Late Quaternary paleotemperatures derived from a speleothem Cango Caves, Cape Province, South Africa. *Quaternary Research* **213**, 203–213.

THACKERAY, J.F. 1987. Late Quaternary environmental changes inferred from small mammalian fauna, southern Africa. *Climatic Change* **10**, 285–305.

TYSON, P.D. 1986. *Climatic Change and Variability in Southern Africa*. Cape Town, Oxford University Press.

VAN ZINDEREN BAKKER, E.M. 1976. The evolution of late Quaternary paleoclimates of southern Africa. *Palaeoecology of Africa* **9**, 160–202.